Frascati Physics Series Vol. 73 (2022)
LFC22: Strong interactions from QCD to new strong dynamics at LHC and Future Colliders
August 29 - September 2, 2022

RESUMMATION OF LARGE ELECTROWEAK TERMS FOR INDIRECT DARK MATTER DETECTION

Martin Vollmann
Institut für Theoretische Physik, Eberhard Karls Universität Tübingen

Abstract

This paper reports on theoretical advances relevant for the indirect detection of TeV-scale Weakly Interacting Massive Particles (WIMPs) as dark matter. Our focus is on the resummation of large electroweak corrections in the endpoint spectrum of gamma rays from WIMP annihilations in the Milky Way, using non-relativistic soft collinear effective field theories. Our results are evaluated in the context of the "wino" and "higgsino" models, achieving next-to-leading-prime accuracy. We also introduce `DM`γ`Spec`, a tool that generates theoretical indirect detection templates for these models, making them readily available for use in gamma-ray telescope analyses.

1 Introduction

Our Universe consists mostly of dark matter - five times more than baryonic matter (stars, etc.) [1]. Despite its abundance, the true nature of dark matter remains unknown. Uncovering its identity is thus a priority area of research in theoretical physics.

The WIMP scenario is an attractive framework that links, rather naturally, the dark matter (DM) problem to the need to extend the Standard Model (SM) of particle physics. WIMPs, which stands for weakly interacting massive particles, decoupled from the primordial plasma at a certain time after being in thermal equilibrium with it. In this hypothesis the observed amount of DM in the Universe depends on the rate of annihilation of these particles, which typically have the same strength as the electroweak interactions. For recent reviews refer to e. g. [2, 3].

The theory space for these wimps is admitely very large, but some predictive scenarios exist. For example, if the DM field is part of an electroweak (EW) multiplet that is electrically neutral after the EW symmetry is broken, large masses of $\mathcal{O}$(TeV) are predicted in this setup [4, 5]. In particular, the

minimal supersymmetric standard model (MSSM) contains fermionic (spin-1/2) EW multiplets that can mix, resulting in the Lightest Supersymmetric (Neutralino) particle (LSP) being a good WIMP DM candidate [6]. Generic neutralinos consist of one Majorana EW triplet (wino), one Dirac doublet (higgsino), and one Majorana singlet (bino). We examine here cases where the mixing is suppressed and the neutralino is mostly wino or higgsino. This is the standard situation in (mini-)split supersymmetric scenarios, e. g. [7, 8].

Detecting heavy DM particles directly or through collider experiments is challenging. However, it may be possible to detect indirect signals, like those from cosmic gamma-ray observations, in the near future [9]. Large quantum effects resulting from the big hierarchies between the DM mass and the masses of the EW gauge bosons and the non-relativistic speeds of DM particles in nearby galaxies, could significantly enhance the DM-induced signals sought by indirect-detection experiments [10, 11].

In this work, we focus on how the aforementioned quantum effects can be accounted for in a systematic way using a suitable effective field theory (EFT). Our focus is on the endpoint of the gamma-ray spectrum, characterized by a prominent line-like bump detectable with current and next-generation telescopes. In particular, we account for the effect of the otherwise negligible emissions of collinear and soft gauge bosons at the endpoint, which in this case play a very important role. Lastly, we introduce `DM`γ`Spec`, a python library to calculate resummed gamma-ray annihilation cross sections for wino/higgsino.

This review is organized as follows: Section 2 covers the basic aspects of the computation of gamma-ray fluxes; Section 3 outlines the EFTs pertinent to this work (NREFT and SCET); Section 4 presents the numerical results; after which we summarize our findings in the conclusions.

2 Phenomenology

Very high energy (VHE) gamma rays from nearby sources, e. g. satellite dwarf galaxies or the Miky-Way halo, can pass through the interstellar medium unimpeded. Therefore, the differential flux (number of photons of energy between E and $E + \mathrm{d}E$ per unit time and area) in a small cone centered in the $\hat{n}$ direction, with a solid angle $\mathrm{d}\Omega_{\hat{n}}$ is given by

$$\mathrm{d}\Phi_\gamma(E) = \mathrm{d}E\,\mathrm{d}\Omega_{\hat{n}} \int_{\mathrm{l.o.s.}} \mathrm{d}s\, q(\hat{n}s) \ , \tag{1}$$

where $q(\hat{n}s)$ is the source function and is given by

$$q(\hat{n}s) = \frac{1}{8\pi m_\chi^2} \rho_{\mathrm{DM}}^2(r(s\hat{n})) \frac{\mathrm{d}\langle\sigma v\rangle}{\mathrm{d}E} \ . \tag{2}$$

In this formula, m_χ is the mass of the DM particle, $\rho_{\mathrm{DM}}(r)$ its density, $\langle\sigma v\rangle$ its velocity-averaged $\chi\chi \to \gamma + X$ annihilation cross section and X is any combination of particles associated with the annihilation process. For a review see e. g. [12]. Assuming a velocity distribution of $\sim \delta^{(3)}(\boldsymbol{v})$, the differential flux can be expressed as the product of an astrophysical "J" factor and the differential annihilation cross-section, with $\langle\sigma v\rangle \simeq \lim_{v\to 0} \sigma v$. For a given observed angular region $\Delta\Omega$, this J-factor is defined as

$$J_{\hat{n}}(\Delta\Omega) = \int_{\Delta\Omega} \mathrm{d}\Omega_{\hat{n}} \int_{\mathrm{l.o.s.}} \mathrm{d}s \rho_{\mathrm{DM}}^2(r(s\hat{n})) \ , \tag{3}$$

Regarding the annihilation process, energy-momentum conservation dictates that the gamma-ray spectrum has a sharp cutopff at[1] $E = m_\chi$. In the idealized case, with e.g. infinite energy-resolution

[1] We use natural units.

detectors, this would appear as a $\gamma\gamma$ line with no width. However, the finite energy resolution of the instrument will cause smearing of this signal. To properly address this, we must consider the more generic annihilation process $\chi\chi \to \gamma + X$, where X denotes all possible unobserved particles with an invariant mass $m_X = 2m_\chi\sqrt{1 - E/m_\chi} \equiv 2m_\chi\sqrt{1-x}$ constrained by the instrument's energy resolution.

3 Non-relativistic and soft collinear effective field theories for DM

In order to gain insight into the complexity of the computation of gamma-ray spectra from TeV-scale DM, consider the fixed-order $\chi\chi \to \gamma\gamma$ amplitude

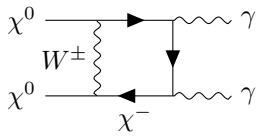

Figure 1: Illustrative Feynman diagram occurring in the $\chi\chi \to \gamma\gamma$ amplitude computation

The Feynman diagram shown above (Fig. 1) has several features that merit special attention. First, due to the fact that the DM is non-relativistic[2], the W-boson t-channel exchange depicted in the figure yields a very large $\sim \alpha_2^2\, m_\chi/m_W$ contribution that invalidates the perturbative expansion. The leading order computation is thus insufficient and the effects of an infinite number of Feynman diagrams has to be included. We thus employ EFT methods to identify and resum large terms that would otherwise invalidate the perturbative expansion. More concretely, in the context of non-relativistic EFTs (NREFT) large terms of $\mathcal{O}(\alpha_2^n m_\chi^n/m_W^n)$ that occur in certain n-loop diagrams ($n = 1, 2, \ldots$) can be resummed by solving a Schrödinger equation with static Yukawa potentials [10, 11, 13], e. g. $V(r) \sim \alpha_{\rm EW}\frac{\mathrm{e}^{-m_W r}}{r}$. Depending on the theory parameters (e. g. DM particle mass), the resummation yields phenomenologically interesting resonant effects (see Fig. 2).

Secondly, the $\chi\chi \to \gamma\gamma$ process is also affected by large Sudakov-like double logarithmic terms $\sim \alpha_2^2\, \log^2(2\, m_\chi/m_W)$. The origin of these terms (and their higher-order counterparts) is also well understood and can be resummed using renormalization-group (RG) running in the context of a soft-collinear EFT (SCET) [14, 15, 16, 17].

Note that although the previous discussion was mostly concerned with the $\chi\chi \to \gamma\gamma$ process, this approach is applicable in the full $\chi\chi \to \gamma + X$ process near the endpoint. More concretely, the NR/SCET EFT for the $\chi\chi \to \gamma + X$ process features the following non-local operators [17]

$$\mathcal{L}_{\rm int} \supset \frac{1}{2m_\chi}\int \mathrm{d}s\,\mathrm{d}t\,\hat{C}_i(s,t)\,\xi^{c\dagger}T_i^{VW}\xi\mathcal{A}^V_{+,\mu}(sn_+)\varepsilon_\perp^{\mu\nu}A^W_{-,\nu}(tn_-)\ , \tag{4}$$

where n_+ and n_- are the four vectors that describe the collinear and anticollinear directions of the process and $\mathcal{A}^V_{\pm,\mu}$ are the associated (anti)collinear SCET building-block fields[3]. The remaining ξ fields are the non-relativistic (here fermionic) two-component spinor DM fields; the T_i^{VW} tensors are constructed in

[2]We adopt the stronger assumption that $v \ll \alpha_{\rm EW}$, where $\alpha_{\rm EW}$ refers to either the α_1 or α_2 couplings in the SM.

[3]The definition of these in terms of light-like Wilson lines is rather involved. We refer to e. g. [18] for a review.

such a way that electroweak symmetries are respected; and $\hat{C}_i(s,t)$ are the Wilson "coefficients" as functions of the t and s parameters that one introduces in the definition of the building-block (anti)collinear vector fields.

The resummation of the Sudakov double logs is completed once renormalization-group equations are solved for the several pieces of the annihilation-process' *factorization formula*. The results depend on the assumptions made about the typical scale of the invariant mass of X. In this work we consider the following two validity regimes. Namely,

- `'nrw'`: $m_X \sim m_W$ or, equivalently $1-x \sim m_W^2/(2\,m_\chi)^2$
- `'int'`: $m_X \sim \sqrt{2\,m_\chi\,m_W}$ or, equivalently $1-x \sim m_W/(2\,m_\chi)$

The case in which m_X is treated as an independent parameter satisfying $2\,m_\chi \gg m_X \gg \sqrt{2\,m_\chi\,m_W}$ or $1-x \gg m_W/(2\,m_\chi)$ (`'wide'`) has been treated in Refs. [16, 19].

4 Resummed pure wino/higgsino spectra

In this section, we explain how to calculate endpoint gamma-ray spectra in pure wino and higgsino models. For the full MSSM, see the recent paper [20]. Details about these models and associated experimental constraints can be found in e. g. [4, 21, 22, 23, 24]. The key features of these are the following:

Wino: a massive fermionic *triplet* is added to the Standard Model (SM). After Electroweak Symmetry Breaking (EWSB), this produces one neutral Majorana particle (χ^0) and one electrically $\chi^\pm$ charged Dirac particle, with a mass splitting of ~ 165 MeV. This is a highly predictive theory, with only one free parameter: the DM mass. Assuming thermal freeze-out, this yields $m_\chi^{\rm wino} \simeq 3$ TeV.

Higgsino: a spin-1/2 EW *doublet* is added to the SM, giving two neutral Majorana particles (χ_1^0, χ_2^0) and a charged Dirac particle ($\chi^\pm$) after EWSB. Like in the wino model, a small mass splitting of ~ 355 MeV between the charged and the neutral particles is induced by EWSB. A dimension-5 operator $(1/\Lambda)\mathcal{O}_H^{\rm dim5}$, where $\Lambda \gg m_\chi$, is required in order to introduce a mass splitting between the two neutral particles. The theory is, thus, characterized by two free parameters: m_χ and Λ (or $\delta m_{\chi^{(0)}}^{h\rm ino}$). In the wimp (thermal freeze-out) hypothesis, $m_\chi^{h\rm ino} \simeq 1$ TeV.

Exploring our resummed spectra further, we stress the obvious fact that χ in $\chi\chi \to \gamma + X$ refers to the LSP (e. g. χ_0^1 in the higgsino model). However, non-relativistic effects may cause the pair of DM particles to virtually transition into, say, a $\chi^+\chi^-$ state. These transitions will play an important role in our factorization formula. We thus introduce the following notation: all electrically neutral combinations of wino/higgsino field pairs will be denoted with the "collective" indices I or $J = (11), (+-), \ldots$ This enables us to express our factorization formula as follows

$$\frac{{\rm d}\langle\sigma v\rangle}{{\rm d}x} = 2\,m_\chi \sum_{I,J} S_{IJ}\Gamma_{IJ}(x)\ . \tag{5}$$

The Sommerfeld factors, S_{IJ}, are independent of x, and account for the resummation of those $\mathcal{O}(\alpha_2^n m_\chi^n/m_W^n)$ terms that are associated to the non-relativistic initial-state kinematics. The associated non-relativistic potentials are known at next-to-leading order [25, 26]. $\Gamma_{IJ}(x)$, however, depends on x

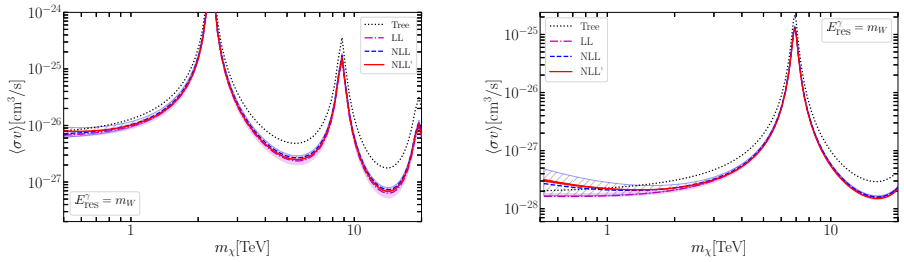

Figure 2: Cumulative $\chi\chi \to \gamma + X$ annihilation cross sections times relative speeds for pure wino (left) and higgsino (right) DM as a function of their particle's mass. Our featured calculation at next-to-leading-log prime accuracy is shown as a solid (red) line. We include, for comparison, the NLL (dashed blue) and LL (dot-dashed magenta) computations with their associated theory-uncertainty bands. For concreteness, $E^{\rm res}_\gamma = m_W$ is assumed (see text for the definitions). Figures taken from [17, 28]

and the factorization regime (i.e. `'nrw'`, `'int'`). In the higgsino model and `'int'` regime, for instance, this reads [17]

$$\Gamma_{IJ}(x) = \frac{1}{(\sqrt{2})^{n_{id}}}\frac{1}{4}\frac{2}{\pi m_\chi}\sum_{i,j} C_i(\mu)C_j^*(\mu) \times Z_\gamma^{WY}(\mu,\nu)\times \int \mathrm{d}\omega \Big(J^{\rm SU(2)}(4m_\chi(m_\chi - E_\gamma - \omega/2),\mu) \times W^{{\rm SU(2)},ij}_{IJ,WY}(\omega,\mu,\nu) + + J^{\rm U(1)}(4m_\chi(m_\chi - E_\gamma - \omega/2),\mu) \times W^{{\rm U(1)},ij}_{IJ,WY}(\omega,\mu,\nu)\Big) \ . \tag{6}$$

As evident in (6), the factorization formula is a product of several pieces. Namely, C_i: Wilson coefficients in momentum space of the SCET; Z_γ and $J^{\mathcal{G}}(m_X^2)$: photon and recoiling jet functions; and $W^{\mathcal{G},ij}_{IJ,WY}$: the soft function (tensor), where $\mathcal{G}$ =U(1) or SU(2). Detailed expressions and proper definitions are given in Refs. [17, 27, 28].

Fig. 2 shows how uncertainties are gradually reduced as we increase the accuracy of our calculations and for large DM masses. In particular, our *next-to-leading logarithmic prime* (NLL') computations are accurate to within a few percent. In this figure, we consider the cumulative cross-section as a function of the variable $E^{\rm res}_\gamma$ which is defined as

$$\langle\sigma v\rangle(E^{\rm res}_\gamma) = \int_{1-E^{\rm res}_\gamma/m_\chi}^{1} \mathrm{d}x' \frac{\mathrm{d}\langle\sigma v\rangle}{\mathrm{d}x'} \ . \tag{7}$$

These figures can also be obtained using a python library `DMySpec` [29] which, among other features, enables the user to numerically evaluate eqs. (5), (6) in the `'int'` and 'nrw' validity regimes. `DMySpec` is also useful for plotting the *complete annihilation spectrum* for generic wino/higgsino DM. This is achieved by matching our results (5), (6) with gamma-ray spectra from parton showers initiated by all possible Born-level 2-2 annihilation processes. The former hold for small values of $1-x$, whereas the latter are valid as long as the collinear approximation is applicable and is given by (5) but instead of using (6) for Γ_{IJ} we use

$$\Gamma^{\rm MC}_{IJ}(x) = \sum_{a,b} (\sigma v)^{(0)}_{(IJ)\,ab} \frac{1}{m_\chi}\frac{\mathrm{d}N^{\rm MC}_{ab\to\gamma+X}}{\mathrm{d}x} \ , \tag{8}$$

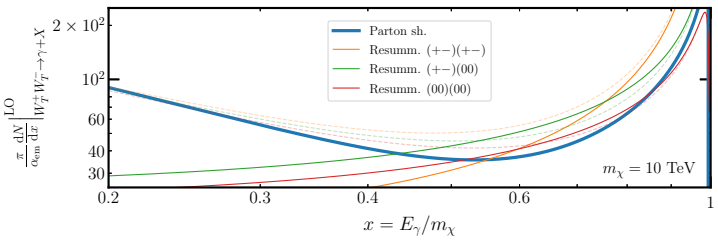

Figure 3: Fixed-order expanded $m_\chi \Gamma_{IJ}/(\sigma v)^{(0)}_{IJ}$ using eq. (6) for the three possible combinations of I and J in the wino model ($m_\chi = 10$ TeV) considered here: in red $I = J = (00)$, etc. Dashed lines are obtained from full Born-level calculations. The (thick) blue line is the result of eq. (9). We use $s_W^2 = 0.222$.

where $a, b = W_T^\pm, Z_T$ or γ. The subscript T means *transverse* here and the upperscript (0) refers to the fact that the cross-section matrices are computed at tree level. For example, in the pure wino case:

$$(\sigma v)^{\text{wino (0)}}_{IJ\,\gamma\gamma} = \frac{s_W^2}{2c_W^2}(\sigma v)^{\text{wino (0)}}_{IJ\,\gamma Z_T} = \frac{s_W^4}{c_W^4}(\sigma v)^{\text{wino (0)}}_{IJ\,Z_T Z_T} = \frac{\pi\alpha_{\text{em}}^2}{m_\chi^2}\delta_{I,(+-)}\delta_{J,(+-)}$$

$$(\sigma v)^{\text{wino (0)}}_{(00)(00)\,W_T W_T} = \sqrt{2}\,(\sigma v)^{\text{wino (0)}}_{(00)(+-)\,W_T W_T} = 2\,(\sigma v)^{\text{wino (0)}}_{(+-)(+-)\,W_T W_T} = \frac{\pi\alpha_2^2}{m_\chi^2}\,,$$

where δ_{IJ} is the Kroenecker delta, α_{em} is the fine-structure constant, and s_W and c_W are respectively the sine and cosines of the Weinberg angle in the SM. The splitting functions $\mathrm{d}N^{\text{MC}}_{X\to\gamma}/\mathrm{d}x$ are obtained from parton showers available in specialized software codes [30, 32, 31, 33].

The matching of these computations is remarkable. In order to understand why this happens, it is useful to compare the (unresummed) $\mathcal{O}(\alpha_{\text{EW}})$ terms associated to each calculation. Specifically, for the parton-shower approach, $\mathrm{d}N^{(0)}_{a,b\to\gamma}/\mathrm{d}x$ vanishes for $(a,b) = (Z_T, Z_T)$, (γZ_T) and $\gamma\gamma$ but is non-zero for $(a,b) = W_T^+ W_T^-$ and is given by [34]

$$\frac{\mathrm{d}N^{(0)}_{W_T^+W_T^-\to\gamma+X}}{\mathrm{d}x} = \frac{2\alpha_{\text{em}}}{\pi}\left[\frac{x}{1-x}\log\frac{4\,m_\chi^2(1-x)^2}{m_W^2} + \left(\frac{1-x}{x} - x(1-x)\right)\log\frac{4\,m_\chi^2}{m_W^2}\right]. \tag{9}$$

Fig. 3 shows this for $m_\chi = 10$ TeV. The other curves shown there are obtained by performing fixed-order expansions in α_{EW} of (6). For $x \lesssim 0.5$, exact one-loop computations match the thick blue line, as expected. At the opposite end of the spectrum ($1 - x \lesssim m_W/m_\chi$ (~ 0.01 for $m_\chi = 10$ TeV), these computations are instead matched by our fixed-order expanded factorization formulas.

5 Conclusions

Indirect detection experiments will probe previously-unexplored regions of WIMP parameter-space in the near future. Radiative electroweak effects are an essential ingredient in the description of indirect-detection signals from TeV-scale dark matter. In particular, a proper treatment of Sudakov-log resummation and Sommerfeld enhancements is crucial in order to reliably assess these heavy WIMP scenarios.

To this end, we devised an EFT (NR/SCET) prescription to obtain fully resummed gamma-ray spectra from generic heavy DM with non-trivial EW multiplicities. In the pure wino and higgsino models we completed this at the NLL' accuracy of $\mathcal{O}(1\%)$. Furthermore, we developed DMγSpec, a tool that makes it easy for Cherenkov telescope experiments to implement our wino/higgsino spectra. Our results show excellent agreement and consistency between its various pieces.

References

1. N. Aghanim *et al.* [Planck], Astron. Astrophys. **641** (2020), A6 [erratum: Astron. Astrophys. **652** (2021), C4] doi:10.1051/0004-6361/201833910 [arXiv:1807.06209 [astro-ph.CO]].

2. G. Arcadi, M. Dutra, P. Ghosh, M. Lindner, Y. Mambrini, M. Pierre, S. Profumo and F. S. Queiroz, Eur. Phys. J. C **78** (2018) no.3, 203 doi:10.1140/epjc/s10052-018-5662-y [arXiv:1703.07364 [hep-ph]].

3. L. Roszkowski, E. M. Sessolo and S. Trojanowski, Rept. Prog. Phys. **81** (2018) no.6, 066201 doi:10.1088/1361-6633/aab913 [arXiv:1707.06277 [hep-ph]].

4. M. Cirelli, N. Fornengo and A. Strumia, Nucl. Phys. B **753** (2006), 178-194 doi:10.1016/j.nuclphysb.2006.07.012 [arXiv:hep-ph/0512090 [hep-ph]].

5. N. Arkani-Hamed, A. Delgado and G. F. Giudice, Nucl. Phys. B **741** (2006), 108-130 doi:10.1016/j.nuclphysb.2006.02.010 [arXiv:hep-ph/0601041 [hep-ph]].

6. G. Jungman, M. Kamionkowski and K. Griest, Phys. Rept. **267** (1996), 195-373 doi:10.1016/0370-1573(95)00058-5 [arXiv:hep-ph/9506380 [hep-ph]].

7. N. Arkani-Hamed, S. Dimopoulos, G. F. Giudice and A. Romanino, Nucl. Phys. B **709** (2005), 3-46 doi:10.1016/j.nuclphysb.2004.12.026 [arXiv:hep-ph/0409232 [hep-ph]].

8. A. Arvanitaki, N. Craig, S. Dimopoulos and G. Villadoro, JHEP **02** (2013), 126 doi:10.1007/JHEP02(2013)126 [arXiv:1210.0555 [hep-ph]].

9. A. Acharyya *et al.* [CTA], JCAP **01** (2021), 057 doi:10.1088/1475-7516/2021/01/057 [arXiv:2007.16129 [astro-ph.HE]].

10. J. Hisano, S. Matsumoto and M. M. Nojiri, Phys. Rev. Lett. **92** (2004), 031303 doi:10.1103/PhysRevLett.92.031303 [arXiv:hep-ph/0307216 [hep-ph]].

11. J. Hisano, S. Matsumoto, M. M. Nojiri and O. Saito, Phys. Rev. D **71** (2005), 063528 doi:10.1103/PhysRevD.71.063528 [arXiv:hep-ph/0412403 [hep-ph]].

12. M. Lisanti, doi:10.1142/9789813149441_0007 [arXiv:1603.03797 [hep-ph]].

13. M. Beneke, C. Hellmann and P. Ruiz-Femenia, JHEP **05** (2015), 115 doi:10.1007/JHEP05(2015)115 [arXiv:1411.6924 [hep-ph]].

14. M. Baumgart, I. Z. Rothstein and V. Vaidya, Phys. Rev. Lett. **114** (2015), 211301 doi:10.1103/PhysRevLett.114.211301 [arXiv:1409.4415 [hep-ph]].

15. M. Bauer, T. Cohen, R. J. Hill and M. P. Solon, JHEP **01** (2015), 099 doi:10.1007/JHEP01(2015)099 [arXiv:1409.7392 [hep-ph]].

16. M. Baumgart, T. Cohen, I. Moult, N. L. Rodd, T. R. Slatyer, M. P. Solon, I. W. Stewart and V. Vaidya, JHEP **03** (2018), 117 doi:10.1007/JHEP03(2018)117 [arXiv:1712.07656 [hep-ph]].

17. M. Beneke, A. Broggio, C. Hasner, K. Urban and M. Vollmann, JHEP **08** (2019), 103 [erratum: JHEP **07** (2020), 145] doi:10.1007/JHEP08(2019)103 [arXiv:1903.08702 [hep-ph]].

18. T. Becher, A. Broggio and A. Ferroglia, Lect. Notes Phys. **896** (2015), pp.1-206 Springer, 2015, doi:10.1007/978-3-319-14848-9 [arXiv:1410.1892 [hep-ph]].

19. M. Baumgart, T. Cohen, E. Moulin, I. Moult, L. Rinchiuso, N. L. Rodd, T. R. Slatyer, I. W. Stewart and V. Vaidya, JHEP **01** (2019), 036 doi:10.1007/JHEP01(2019)036 [arXiv:1808.08956 [hep-ph]].

20. M. Beneke, S. Lederer and C. Peset, JHEP **01** (2023), 171 doi:10.1007/JHEP01(2023)171 [arXiv:2211.14341 [hep-ph]].

21. J. Fan and M. Reece, JHEP **10** (2013), 124 doi:10.1007/JHEP10(2013)124 [arXiv:1307.4400 [hep-ph]].

22. T. Cohen, M. Lisanti, A. Pierce and T. R. Slatyer, JCAP **10** (2013), 061 doi:10.1088/1475-7516/2013/10/061 [arXiv:1307.4082 [hep-ph]].

23. K. Kowalska and E. M. Sessolo, Adv. High Energy Phys. **2018** (2018), 6828560 doi:10.1155/2018/6828560 [arXiv:1802.04097 [hep-ph]].

24. R. T. Co, B. Sheff and J. D. Wells, Phys. Rev. D **105** (2022) no.3, 035012 doi:10.1103/PhysRevD.105.035012 [arXiv:2105.12142 [hep-ph]].

25. M. Beneke, R. Szafron and K. Urban, JHEP **02** (2021), 020 doi:10.1007/JHEP02(2021)020 [arXiv:2009.00640 [hep-ph]].

26. K. Urban, JHEP **10** (2021), 136 doi:10.1007/JHEP10(2021)136 [arXiv:2108.07285 [hep-ph]].

27. M. Beneke, A. Broggio, C. Hasner and M. Vollmann, Phys. Lett. B **786** (2018), 347-354 [erratum: Phys. Lett. B **810** (2020), 135831] doi:10.1016/j.physletb.2018.10.008 [arXiv:1805.07367 [hep-ph]].

28. M. Beneke, C. Hasner, K. Urban and M. Vollmann, JHEP **03** (2020), 030 doi:10.1007/JHEP03(2020)030 [arXiv:1912.02034 [hep-ph]].

29. M. Beneke, K. Urban and M. Vollmann, Phys. Lett. B **834** (2022), 137248 doi:10.1016/j.physletb.2022.137248 [arXiv:2203.01692 [hep-ph]].

30. M. Cirelli, G. Corcella, A. Hektor, G. Hutsi, M. Kadastik, P. Panci, M. Raidal, F. Sala and A. Strumia, JCAP **03** (2011), 051 [erratum: JCAP **10** (2012), E01] doi:10.1088/1475-7516/2012/10/E01 [arXiv:1012.4515 [hep-ph]].

31. T. Bringmann and J. Edsjö, PoS **CompTools2021** (2022), 038 doi:10.22323/1.409.0038 [arXiv:2203.07439 [hep-ph]].

32. G. Belanger, F. Boudjema, A. Pukhov and A. Semenov, Comput. Phys. Commun. **185** (2014), 960-985 doi:10.1016/j.cpc.2013.10.016 [arXiv:1305.0237 [hep-ph]].

33. T. Bringmann *et al.* [GAMBIT Dark Matter Workgroup], Eur. Phys. J. C **77** (2017) no.12, 831 doi:10.1140/epjc/s10052-017-5155-4 [arXiv:1705.07920 [hep-ph]].

34. P. Ciafaloni, D. Comelli, A. Riotto, F. Sala, A. Strumia and A. Urbano, JCAP **03** (2011), 019 doi:10.1088/1475-7516/2011/03/019 [arXiv:1009.0224 [hep-ph]].